Acta Cryst. (1994). B50, 13–22

Structure Determination of the Ferroelastic Phase of $K_3Na(CrO_4)_2$ at 200 and 230 K and the Redetermination of its Parent Phase at 290 K

BY J. FÁBRY,* T. BRECZEWSKI AND G. MADARIAGA

Departamento de Física de la Materia Condensada, Facultad de Ciencias, Universidad del Pais Vasco, Apdo. 644, 48080 *Bilbao, Spain*

(*Received* 6 *January* 1993; *accepted* 3 *August* 1993)

Abstract

$K_3Na(CrO_4)_2$, $M_r = 372.27$, λ(Mo $K\alpha$) = 0.71073 Å, two crystals were measured; crystal *A* at 290, 230 and 200 K and crystal *B* at 200 K. Both crystals were twinned in the room-temperature phase ($P\bar{3}m1$); the twinning operation $\hat{T}$ was the twofold axis parallel with the *c* axis. After the phase transition (T_{trans} = 239 K) into the ferroelastic phase each domain which is present in the high-temperature phase gives rise to three domains with 120° orientation. Thus, the diffraction pattern of the low-temperature phase can be formally treated as if it were composed of six domains with 60° orientation. Crystal data: crystal *A*: $T = 290$ K, trigonal, $P\bar{3}m1$, $a = 5.857$ (3), $c = 7.521$ (2) Å, $V = 223.4$ Å^3, $\mu = 38.33$ cm^{-1}, $Z = 1$, $F(000) = 180$, $D_x = 2.766$ g cm^{-3}, $R = 0.0145$ for 238 observed reflections. $T = 230$ K, monoclinic, $C2/c$, $a = 10.128$ (3), $b = 5.8437$ (5), $c = 15.022$ (2) Å, $\beta = 89.97$ (2)°, $V = 889.1$ Å^3, $\mu = 38.53$ cm^{-1}, $Z = 4$, $F(000) = 720$, $D_x = 2.780$ g cm^{-3}, $R = 0.0331$ for 2078 observed reflections. $T = 200$ K, monoclinic, $C2/c$, $a = 10.117$ (1), $b = 5.843$ (2), $c = 15.024$ (2) Å, $\beta = 89.967$ (7)°, $V = 888.1$ Å^3, $\mu = 38.57$ cm^{-1}, $Z = 4$, $F(000) = 720$, $D_x = 2.783$ g cm^{-3}. Crystal *A*: $R = 0.0315$ for 2149 observed reflections; crystal *B*: $R = 0.0288$ for 2045 observed reflections. The respective high- and low-temperature phases of $K_3Na(CrO_4)_2$ and $K_3Na(SeO_4)_2$ are isomorphous. By analogy with $K_3Na(SeO_4)_2$ the title compound undergoes a ferroelastic phase transition from a $\bar{3}m1$ point group to $2/m$ and the *c* axis of the ferroelastic phase which is originally coincident with the trigonal axis doubles its length. On the other hand, contrary to $K_3Na(SeO_4)_2$, only twinned single crystals did not crack during this phase transition. The phase transition is accompanied by shifts of two crystallographically independent K^+ cations, as well as by shift and tilting of $[CrO_4]^{2-}$. The phase transition affects mainly the environment of K(2) which is the most loosely bound cation in the structure. The atomic displacements from the positions in the high-temperature phase are significantly larger at 200 than at 230 K, thus indicating a continuous phase transition.

Introduction

$K_3Na(CrO_4)_2$ undergoes a ferroelastic phase transition at 239 K (Krajewski, Mroz, Piskunowicz & Breczewski, 1990). The ferroelastic properties of the low-temperature phase were confirmed by the direct observation of domains which were reorientable under mechanical stress. Optical observation, DTA experiments, measurements with a miniature torsional pendulum and dielectric properties (*ibid.*) led to the conclusion that the phase transition is of order–disorder type and the crystal classes of the high- and low-temperature phases are $\bar{3}m1$ and $2/m$, respectively. Mroz, Kiefte, Clouter & Tuszynski (1991) concluded from the Brillouin scattering studies that the present phase transition is a weak first-order one. The structural study of the room-temperature phase ($P\bar{3}m1$) (Madariaga & Breczewski, 1990) determined that the structure is isomorphous to $K_3Na(SO_4)_2$ (Okada & Ossaka, 1980).

Recently, the structures of the high- and low-temperature phases of the analogous compound $K_3Na(SeO_4)_2$ have been solved (Fábry, Breczewski & Petricek, 1993). This structure determination revealed that the high-temperature phase of $K_3Na(SeO_4)_2$ is isomorphous to the room-temperature phases of $K_3Na(SO_4)_2$ and $K_3Na(CrO_4)_2$. During the phase transition of $K_3Na(SeO_4)_2$ into the low-temperature phase ($C2/c$) the *c* axis doubles its length and the mirror plane is replaced by the glide plane *c*.

Precession photographs of $K_3Na(CrO_4)_2$ showed the analogous doubling of the *c* axis below the phase transition (Fábry, Breczewski & Petricek, 1993) and systematic extinctions $00l$, $l = 2n + 1$. Trial diffractometer measurements revealed that the intensities of some reflections, h,k,l, $l = 2n + 1$, rose considerably

* On leave of absence from the Institute of Physics of the Czechoslovak Academy of Sciences, Na Slovance 2, 180 40 Praha 8, Czechoslovakia. Correspondence should be directed to the address given in this footnote.

on decreasing the temperature 30 K below the transition point. The dielectric permittivity in the ⟨1,0,0⟩ direction (expressed in the lattice of the high-temperature phase) changes continuously (Krajewski, Mroz, Piskunowicz & Breczewski, 1990) in this temperature region.

The aim of the present work was to determine the structure of the low-temperature phase in this temperature region.

Experimental

The yellow–orange crystals of the title compound were grown from an aqueous stoichiometric solution of K_2CrO_4 and Na_2CrO_4. Two crystals were used in this experiment. Crystal *B* had the shape of a hexagonal column 0.1 mm thick and 0.26 mm long, while crystal *A* which was cut from a larger crystal had the shape of a rectangular parallelepiped of dimensions 0.22 × 0.27 × 0.30 mm. Crystal *A* was examined at 200, 230 and 290 K and crystal *B* at 200 K.

Data collection was performed on an Enraf–Nonius CAD-4 diffractometer which was equipped with a graphite-plane monochromator; the samples were cooled by a stream of nitrogen gas (Cosier & Glazer, 1986) with a precision of 1 K.

Unlike the crystal at room temperature, which is a true merohedral twin, the reflections of the ferroelastic phase need not necessarily exactly overlap, and the lattice parameters determined from the multiply twinned monocrystal reflections of the ferroelastic phase are biased by this systematic error. Thus, the single-crystal diffractometer will tend to centre reflections at the centroid of the bundle of superimposed diffractions. For these reasons we report here the unit-cell parameters of the ferroelastic phase at 200 and 230 K which were obtained from powder-diffraction measurements. These experiments were performed on a Stoe focusing monochromatic beam transmission diffractometer equipped with a linear-position detector. The powdered sample was inserted into a Lindemann capillary of diameter 0.3 mm. The measured region was 5.00–84.89° (2θ). λ(Cu $K\alpha_1$) = 1.54056 Å. Figures of merit $F(N_{obs}/\Delta 2\theta_{average})$ after least-squares refinement of lattice parameters were $F(34/0.005) = 21.6$ and $F(35/0.004) = 27.9$ for 200 and 230 K, respectively.

With the exception of the two twinned crystals, the measurement of which is reported here, all single-crystal samples cracked during the phase transition. Crystal *A* was cooled down to 230 K first and then, because of breakdown of the cooling device, quickly heated to room temperature. It was then measured at room temperature and cooled down to 230 K again (this experiment is reported here). A further breakdown of the cooling device terminated the experiment at this temperature and the crystal was then cooled down to 200 K. These temperature jumps, however, did not apparently affect either the widths or intensities of the reflections which were used for determination of the orientation matrix. ω/θ plots indicated that an $\omega/2\theta$ scan was most appropriate for crystal *A* and an ω scan for crystal *B*.

The absorption correction (Gaussian integration) together with a correction for the variation of the standard-reflection intensities were provided by the program system *XRAY*72 (Stewart *et al.*, 1972); Lp correction, calculation of structure factors and their e.s.d.'s together with their averaging with respect to the symmetry were carried out by the conversion program of the *SDS* system (Petricek & Maly, 1988). The square roots of the intensities of the trigonal phase measured at 290 K were averaged with regard to the crystal class symmetry operations while the square roots of the intensities of the phases measured at 230 and 200 K were averaged with respect to the centre of symmetry. (For the calculation of Fourier syntheses of the low-temperature phases, however, a set of symmetry-independent reflections was selected.) The *SDS* program performed the rest of the calculations except the bond-length correction for the temperature movement which was carried out by the program *PARST* (Nardelli, 1983). Scattering factors including anomalous dispersion corrections were taken from Cromer & Mann (1968) and *International Tables for X-ray Crystallography* (1974, Vol. IV).

The structure of the 290 K phase and the twinning operation, which is a twofold axis parallel with the *c* axis, were determined by the solution of the Patterson synthesis.

The heights of the Cr—O(2) peaks (or more precisely the integrated values of the squared electron density within these peaks) of the Patterson synthesis also yield information about the ratio of component twins. As a consequence of the ferroeleastic phase transition into the supposed $C2/c$ space group, each twin component of the high-temperature phase gives rise to three domains with 120° mutual orientation. Thus, the whole crystal below the phase-transition point may be treated as if it were composed from six domains with 60° orientation (Table 2). Provided that this is the transition from the trigonal parent phase into the monoclinic ferroelastic phase the sum of the domain fractions with 120° mutual orientation should equal the values of the respective twin fractions of the parent phase at 290 K (the effect of mutual-domain shielding is assumed not to be pronounced). However, this condition regarding the sum of domain fractions would not be valid for the transition into the triclinic structure because each parent domain from the room-temperature phase would split into six domains.

Table 1. *Data collection and refinement parameters for* $K_3Na(CrO_4)_2$

Crystal	*A*	*A*	*A*	*B*
Temperature (K)	290 (1)	230 (1)	200 (1)	200 (1)
Scan type	$\omega/2\theta$	$\omega/2\theta$	$\omega/2\theta$	ω
ω-scan width (°)	1.10 + 0.35tan θ	1.00 + 0.35tan θ	1.00 + 0.35tan θ	1.00 + 0.35tan θ
Horizontal aperture (mm)	2.80 + 0.15tan θ	2.80 + 0.15tan θ	2.80 + 0.15tan θ	1.60 + 1.95tan θ
Vertical aperture (mm)	4	4	4	4
Minimal/maximal scan speed (° min^{-1})	0.824, 5.493	0.749, 5.493	0.749, 5.493	0.867, 5.493
Maximal final scan time (s)	120	120	120	120
Measured region θ (°)	≤ 28	≤ 28	≤ 28	≤ 28
h range	⟨−7,7⟩	⟨−13,13⟩ and ⟨−10,3⟩	⟨−13,13⟩	⟨−13,13⟩
k range	⟨−7,7⟩	⟨0,7⟩ and ⟨−4,6⟩	⟨−7,7⟩	⟨−7,7⟩
l range	⟨−9,9⟩	⟨−19,19⟩ and ⟨−19,−11⟩	⟨−19,19⟩	⟨−19,19⟩
Average positive and negative deviations (%) from the mean intensities of five standards	−2.2; 2.1	−3.8; 4.6	−3.5; 3.9	−6.7; 7.0
Monitoring interval (s)	3600	3600	3600	3600
No. of measured reflections	2187	2561	4295	4301
No. of observed reflections [$I \geq 3\sigma(I)$]	2187	2454	4238	4126
Averaging: No. of all/obs. reflections	238/238	2159/2078	2149/2118	2153/2045
Estimated R factors: all/obs. reflections	0.008/0.008	0.014/0.013	0.011/0.011	0.023/0.021
R_{int}	0.056	0.030	0.030	0.017
Minimal/maximal transmission factors	0.3257/0.4350	0.3237/0.4320	0.3237/0.4320	0.6821/0.7752
Extinction correction/isotropic Lorentzian distribution (g)	0.24 (6) × 10^{-4}	0.17 (1) × 10^{-4}	0.068 (8) × 10^{-4}	—
Domain fractions:				
f_1	0.468 (3)	0.184 (3)	0.167 (3)	0.143 (2)
f_2	0.532 (3)	0.180 (3)	0.142 (3)	0.133 (2)
f_3		0.124 (3)	0.163 (2)	0.126 (2)
f_4		0.160 (3)	0.195 (3)	0.205 (2)
f_5		0.134 (3)	0.119 (2)	0.184 (2)
f_6		0.218 (3)	0.214 (3)	0.209 (2)
$f_1 + f_3 + f_5$		0.442	0.449	0.453
$f_2 + f_4 + f_6$		0.558	0.551	0.547
No. of refined parameters	21	67	67	71
Weighting scheme: w^{-1} =	$\sigma^2(F_o) + (0.01\|F_o\|)^2$	$\sigma^2(F_o) + (0.01\|F_o\|)^2$	$\sigma^2(F_o) + (0.01\|F_o\|)^2$	$\sigma^2(F_o) + (0.01\|F_o\|)^2$
R for all reflections	0.0145	0.0341	0.0319	0.0305
R for observed reflections only	0.0145	0.0331	0.0315	0.0288
wR for all reflections	0.0238	0.0438	0.0410	0.0363
wR for observed reflections only	0.0238	0.0436	0.0409	0.0357
S	1.847	2.357	2.516	1.470
$\Delta\rho^1_{max}$ (e Å^{-3})	0.782	5.192	9.294	4.115
$\Delta\rho^1_{min}$ (e Å^{-3})	−1.707	−7.445	−10.99	−7.743
$\Delta\rho^2_{max}$ (e Å^{-3})	0.348	0.835	1.447	0.705
$\Delta\rho^2_{min}$ (e Å^{-3})	−0.542	−0.904	−1.698	−0.985
$(\Delta/\sigma)_{max}$	≤0.01	≤0.02	≤0.02	≤0.02

The starting model which was used for the refinement of the low-temperature structures was calculated from the structure determined at 290 K. The initial values of the domain fractions were calculated either from the ratio of the heights of the appropriate Cr—O peaks of the Patterson map (crystal *B*) or from the result of the structure determination at 290 K (crystal *A*), assuming an equal distribution of domain fractions within each respective 120° domain pattern.

In the beginning of the refinement of the low-temperature phase the geometry of the $[CrO_4]^{2-}$ anion was kept fixed. The inclusion of extinction corrections into the refinement (type I, isotropic Lorentzian distribution; Becker & Coppens, 1974) proved to be significant for crystal *A*.

The difference Fourier synthesis $\Delta\rho = V^{-1}\sum_h \Delta F(\mathbf{h})\exp(-2\pi i\mathbf{hr})$, where $\Delta F(\mathbf{h}) = |F_o|/\mathrm{Sc} - |F_c(\mathbf{h})|$ for a single-domain crystal (Sc is a general scaling factor), is modified for a multiply twinned crystal which is composed from N domains (f_i is the ith domain fraction, $|F_c|_i$ are calculated moduli of structure factors of the ith domain) as follows:

$$\Delta F(\mathbf{h}) = \left[\frac{\frac{|F_o|^2}{\mathrm{Sc}^2} - \sum_{i=2}^{N} f_i|F_c|^2_i}{f_1}\right]^{1/2} - |F_c|_1.$$

Compared with the structure refinement of a single-domain crystal which converges to similar R-factor values, this modified difference Fourier synthesis inevitably results in higher electron-density values (the pertinent residuals $\Delta\rho$, which are given in Table 1, have the superscript '1').

A referee pointed out that there exists another possibility of calculation of the residual electron densitites which is based on the relation $|F_o|_1 = (Y_o/Y_c)^{1/2}|F_c|_1$, where Y_o and Y_c are the scaled observed and calculated intensities; $|F_o|_1$ and $|F_c|_1$ are 'observed' and calculated absolute values of structure factors, respectively. Unlike the first modification of the difference electron-density calcu-

lation the second assumes that disagreement between $(Y_o)^{1/2}$ and $(Y_c)^{1/2}$ is equally distributed among all domains. The corresponding residuals (Table 1) of the latter modification of the electron-density calculation have the superscript '2'.

The pseudotrigonal axis which links the pseudosymmetrically related atoms is coincident with the reciprocal axis c^*. In order to calculate the atomic displacement vectors Δ (Abrahams & Keve, 1971) which link the pseudosymmetrically related atoms, the atomic positions were transformed into an orthogonal coordinate system, rotated by 120 and 240° along the c^* direction (see Table 2) and consecutively transformed into the fractional coordinates of the orthogonal unit cell (Fig. 1 and Tabel 2). The values of Δ are given in Table 10.

Other relevant information about the experiment and refinement is given in Table 1.*

Discussion

The atomic coordinates and temperature factors are given in Tables 3–5 and Figs. 2–7 depict the structure at different temperatures. Table 6 lists the relevant interatomic distances and angles.

Comparison with the previous structure determination of the room-temperature phase of $K_3Na(CrO_4)_2$ (Madariaga & Breczewski, 1990) which was performed on a non-twinned monocrystal reveals that the atomic coordinates are in good accordance, mostly within the interval of 2 e.s.d.'s with the exception of the Cr z coordinate (~10 e.s.d.'s). The difference between the two results regarding this fractional coordinate is about 0.001, which corresponds to 0.0075 Å.

The temperature factors of the Cr atom of crystal A measured at 230 K became non-positive definite (the amplitude of the thermal ellipsoid in the ⟨0,1,0⟩ direction was negative). Similarly, the amplitude of the thermal ellipsoid of the Cr atom (crystal A; 200 K) was improbably small in the same direction. Thus, the Cr atoms in the low-temperature phases of crystal A were refined isotropically.

The isotropic refinement of the Cr atom increased the R-factor values by 0.003 and 0.001 for 230 and 200 K, respectively. The atomic positions were slightly affected: for 230 and 200 K the greatest difference concerned the y coordinate of the Cr atom, which was about 15 and 10 pertinent e.s.d.'s,

* Lists of structure factors have been deposited with the British Library Document Supply Centre as Supplementary Publication No. SUP 71387 (87 pp.). Copies may be obtained through The Technical Editor, International Union of Crystallography, 5 Abbey Square, Chester CH1 2HU, England. [CIF reference: AL0554]

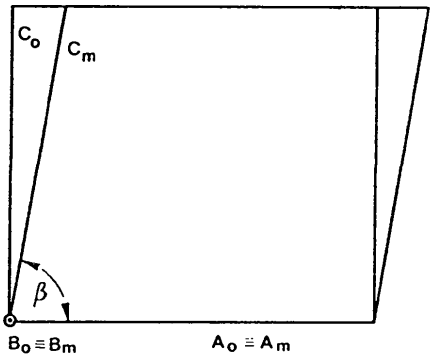

Fig. 1. Relation between the monoclinic and orthogonal unit cells. C_o is the common axis for the three domains about which the 120 and 240° rotations take place, corresponding to ferroelastic switching.

Table 2. *Relevant transformations and relations used in the structure determination of the low-temperature phase of* $K_3Na(CrO_4)_2$

(*a*) Relations for superposition of indices from pertinent domains; index numbers n (n = 1, 2, 3, 4, 5) denominate overlapping reflections from domains which are rotated with respect to the basic domain by $n \times 60°$ degrees in an anticlockwise direction

$$\begin{bmatrix} h \\ k \\ l \end{bmatrix}^1 = \begin{bmatrix} \frac{1}{2} & \frac{3}{2} & 0 \\ -\frac{1}{2} & \frac{1}{2} & 0 \\ 0 & 0 & 1 \end{bmatrix} \begin{bmatrix} h \\ k \\ l \end{bmatrix} \quad \begin{bmatrix} h \\ k \\ l \end{bmatrix}^2 = \begin{bmatrix} -\frac{1}{2} & \frac{3}{2} & 0 \\ -\frac{1}{2} & -\frac{1}{2} & 0 \\ 0 & 0 & 1 \end{bmatrix} \begin{bmatrix} h \\ k \\ l \end{bmatrix}$$

$$\begin{bmatrix} h \\ k \\ l \end{bmatrix}^3 = \begin{bmatrix} -1 & 0 & 0 \\ 0 & -1 & 0 \\ 0 & 0 & 1 \end{bmatrix} \begin{bmatrix} h \\ k \\ l \end{bmatrix} \quad \begin{bmatrix} h \\ k \\ l \end{bmatrix}^4 = \begin{bmatrix} -\frac{1}{2} & -\frac{3}{2} & 0 \\ \frac{1}{2} & -\frac{1}{2} & 0 \\ 0 & 0 & 1 \end{bmatrix} \begin{bmatrix} h \\ k \\ l \end{bmatrix}$$

$$\begin{bmatrix} h \\ k \\ l \end{bmatrix}^5 = \begin{bmatrix} \frac{1}{2} & -\frac{3}{2} & 0 \\ \frac{1}{2} & \frac{1}{2} & 0 \\ 0 & 0 & 1 \end{bmatrix} \begin{bmatrix} h \\ k \\ l \end{bmatrix}$$

(*b*) Transformation of the fractional coordinates (x_m, y_m, z_m) expressed in the standard monoclinic unit cell (A_m, B_m, C_m, β) into the absolute coordinates X_o, Y_o, Z_o) (Å) of the Cartesian system (see also Fig. 1)

$$\begin{pmatrix} X_o \\ Y_o \\ Z_o \end{pmatrix} = \begin{pmatrix} A_m & C_m\cos\beta \\ & B_m \\ & C_m\sin\beta \end{pmatrix} \begin{pmatrix} x_m \\ y_m \\ z_m \end{pmatrix}$$

(*c*) Expressions for calculations of absolute coordinates related by rotation of 120° ('A indices') and 240° ('B indices') about the c^* axis in an anticlockwise direction

$$\begin{pmatrix} X_A \\ Y_A \\ Z_A \end{pmatrix} = \begin{pmatrix} -\frac{1}{2} & -\frac{\sqrt{3}}{2} & \\ \frac{\sqrt{3}}{2} & -\frac{1}{2} & \\ & & 1 \end{pmatrix} \begin{pmatrix} X_o \\ Y_o \\ Z_o \end{pmatrix} \quad \begin{pmatrix} X_B \\ Y_B \\ Z_B \end{pmatrix} = \begin{pmatrix} -\frac{1}{2} & \frac{\sqrt{3}}{2} & \\ -\frac{\sqrt{3}}{2} & -\frac{1}{2} & \\ & & 1 \end{pmatrix} \begin{pmatrix} X_o \\ Y_o \\ Z_o \end{pmatrix}$$

(*d*) Transformation of lattice parameters from monoclinic into the orthogonal unit cell

$$\begin{pmatrix} A_o \\ B_o \\ C_o \end{pmatrix} = \begin{pmatrix} 1 & & \\ & 1 & \\ & & \sin\beta \end{pmatrix} \begin{pmatrix} A_m \\ B_m \\ C_m \end{pmatrix}$$

Table 3. *Atomic positional parameters and anisotropic thermal parameters* U_{ij} ($\times 10^5$ Å^2) *(with e.s.d.'s in parentheses) of the high-temperature phase of* $K_3Na(CrO_4)_2$ (290 K)

The anisotropic temperature factors are of the form: $\exp[-2\pi^2(U_{11}h^2a^{*2} + U_{22}k^2b^{*2} + U_{33}l^2c^{*2} + 2U_{12}hka^*b^* + 2U_{13}hla^*c^* + 2U_{23}klb^*c^*)]$.

	x	y	z	$U(11)$	$U(22)$	$U(33)$	$U(12)$	$U(13)$	$U(23)$
Cr	$\frac{1}{3}$	$\frac{2}{3}$	0.27344 (7)	1095 (24)	1095 (24)	1100 (34)	547 (12)	0	0
K(1)	$\frac{1}{3}$	$\frac{2}{3}$	0.8326 (1)	2009 (28)	2009 (28)	1587 (50)	1004 (14)	0	0
K(2)	0	0	$\frac{1}{2}$	4253 (54)	4253 (54)	1913 (73)	2126 (27)	0	0
Na	0	0	0	1440 (59)	1440 (59)	1621 (91)	720 (29)	0	0
O(1)	$\frac{1}{3}$	$\frac{2}{3}$	0.4877 (7)	5845 (151)	5845 (151)	1376 (130)	2920 (76)	0	0
O(2)	0.18136 (15)	0.36272 (30)	0.1972 (3)	2628 (66)	1691 (70)	4182 (88)	846 (35)	−497 (50)	−993 (100)

Table 4. *Atomic positional parameters and thermal parameters* U_{ij}/U_{iso} ($\times 10^5$ Å^2) *(with e.s.d.'s in parentheses) of the low-temperature phase of* $K_3Na(CrO_4)_2$ (230 K), *crystal A*

The anisotropic temperature factors are of the form: $\exp[-2\pi^2(U_{11}h^2a^{*2} + U_{22}k^2b^{*2} + U_{33}l^2c^{*2} + 2U_{12}hka^*b^* + 2U_{13}hla^*c^* + 2U_{23}klb^*c^*)]$. The isotropic factor is of the form: $\exp(-8\pi^2U_{iso}\sin^2\theta/\lambda^2)$.

	x	y	z	$U(11)/U_{iso}$	$U(22)$	$U(33)$	$U(12)$	$U(13)$	$U(23)$
Cr	0.1663 (2)	0.49528 (3)	0.13696 (3)	830 (10)					
K(1)	0.1671 (4)	0.49446 (6)	0.41669 (4)	2045 (107)	1223 (89)	1027 (32)	−36 (17)	−28 (129)	70 (10)
K(2)	0	0.9836 (1)	$\frac{1}{4}$	4220 (147)	2734 (90)	1252 (40)	0	34 (117)	0
Na	0	0	0	2199 (307)	105 (231)	1111 (63)	−26 (43)	−49 (373)	55 (21)
O(1)	0.166 (2)	0.5133 (3)	0.2441 (2)	4868 (428)	4238 (322)	877 (90)	359 (190)	−200 (348)	−145 (64)
O(2)	0.0890 (9)	0.719 (1)	0.0943 (6)	2698 (364)	1449 (274)	3035 (190)	406 (188)	−183 (251)	608 (169)
O(3)	0.0891 (9)	0.261 (1)	0.1044 (6)	2694 (309)	1306 (206)	3315 (192)	−326 (161)	−106 (223)	−664 (161)
O(4)	0.317 (1)	0.4905 (7)	0.097 (1)	1512 (26)	2147 (295)	3334 (334)	3 (203)	1268 (276)	405 (180)

Table 5. *Atomic positional parameters and anisotropic thermal parameters* U_{ij}/U_{iso} ($\times 10^5$ Å^2) *(with e.s.d.'s in parentheses) of the low-temperature phase of* $K_3Na(CrO_4)_2$ (200 K)

The line headed by the atomic symbol applies for crystal *B*, the line below for crystal *A*. The anisotropic temperature factors are of the form: $\exp[-2\pi^2(U_{11}h^2a^{*2} + U_{22}k^2b^{*2} + U_{33}l^2c^{*2} + 2U_{12}hka^*b^* + 2U_{13}hla^*c^* + 2U_{23}klb^*c^*)]$. The isotropic temperature factor is of the form: $\exp(-8\pi^2U_{iso}\sin^2\theta/\lambda^2)$.

	x	y	z	$U(11)/U_{iso}$	$U(22)$	$U(33)$	$U(12)$	$U(13)$	$U(23)$
Cr	0.1657 (2)	0.49142 (6)	0.13678 (3)	788 (61)	866 (57)	812 (21)	8 (14)	−179 (68)	16 (10)
	0.1653 (1)	0.49082 (4)	0.13670 (3)	680 (10)					
K(1)	0.1685 (2)	0.48967 (9)	0.41609 (4)	1642 (91)	1322 (79)	1181 (30)	−22 (20)	−190 (91)	110 (14)
	0.1683 (2)	0.48908 (8)	0.41610 (4)	1632 (82)	1085 (64)	950 (30)	−43 (20)	35 (95)	101 (12)
K(2)	0	0.9701 (2)	$\frac{1}{4}$	3120 (124)	2484 (71)	1419 (38)	0	112 (84)	0
	0	0.9684 (2)	$\frac{1}{4}$	3103 (134)	2186 (66)	1185 (35)	0	185 (76)	0
Na	0	0	0	610 (243)	1632 (276)	1258 (69)	−47 (63)	−326 (253)	89 (32)
	0	0	0	953 (273)	1071 (271)	934 (64)	57 (57)	176 (293)	105 (29)
O(1)	0.169 (1)	0.5232 (3)	0.2439 (2)	4779 (318)	3156 (205)	1037 (87)	177 (191)	−122 (243)	−246 (80)
	0.170 (1)	0.5245 (3)	0.2438 (2)	4419 (315)	2931 (190)	950 (86)	168 (217)	−454 (207)	−210 (83)
O(2)	0.0872 (5)	0.7092 (7)	0.0912 (3)	1263 (240)	1755 (180)	2833 (207)	470 (129)	−149 (200)	612 (174)
	0.0866 (6)	0.7082 (7)	0.0903 (3)	1500 (247)	1456 (168)	2623 (186)	354 (125)	55 (201)	632 (168)
O(3)	0.0879 (5)	0.2545 (7)	0.1095 (4)	1594 (280)	1629 (210)	2764 (181)	−470 (147)	−164 (178)	−446 (121)
	0.0870 (5)	0.2541 (7)	0.1098 (3)	1589 (273)	1501 (204)	2693 (176)	−533 (155)	−274 (192)	−265 (121)
O(4)	0.3169 (5)	0.4823 (8)	0.0951 (7)	1220 (171)	2359 (222)	2599 (323)	−27 (173)	712 (211)	250 (183)
	0.3168 (5)	0.4810 (9)	0.0956 (7)	1063 (157)	2230 (191)	2248 (263)	58 (175)	754 (199)	107 (175)

respectively. This corresponds to the approximate difference of 0.0005 fractional units (0.003 Å).

The structure determination of crystal *B* at 200 K should be preferred as the temperature factors seem to be normal. The Cr—O bond-length correction – 'riding motion' – which was calculated for the structure measured at 290 K (crystal *A*) and for crystal *B* measured at 200 K (Busing & Levy, 1964), resulted in a more even distribution of Cr–O distances.

A serious experimental problem concerns the influence of a non-homogeneous domain distribution on the measured intensities. The structure determination of crystal *B* should be less affected by this phenomenon because it is elongated along the pseudo-trigonal axis of the low-temperature phase about which the twinning operations takes place – see the crystal dimensions in the beginning of the *Experimental*. (The diffractometer φ-axis was approximately parallel to the crystal's *c* axis.)

In order to assess the influence of the domain distribution on structural parameters, additional refinements of the room-temperature phase (crystal *A*) were performed on the data in 60° segments and its inversion counterparts of the measured reciprocal

Table 6. *Selected interatomic distances* (Å) *and angles* (°) *of the low- and high-temperature phases*

Values in brackets apply to Cr—O distances corrected for thermal motion.

Crystal	*A*		*A*	*A*	*B*
Temperature (K)	290		230	200	200
Coordination of K(1)					
K(1)—O(1)	2.595 (5)	K(1)—O(1)	2.595 (3)	2.597 (3)	2.594 (3)
K(1)—O(2^{v})	2.940 (2)	K(1)—O(2^{i})	2.912 (9)	2.881 (6)	2.890 (5)
K(1)—O(2^{vi})	2.940 (2)	K(1)—O(2^{iv})	2.953 (9)	2.975 (6)	2.968 (5)
K(1)—O(2^{ii})	2.940 (2)	K(1)—O(3^{iv})	2.937 (9)	2.945 (6)	2.936 (5)
K(1)—O(2^{iii})	2.940 (2)	K(1)—O(3^{i})	2.949 (9)	2.952 (6)	2.960 (5)
K(1)—O(2^{viii})	2.940 (2)	K(1)—O(4^{v})	2.911 (4)	2.884 (6)	2.887 (5)
K(1)—O(2^{ix})	2.940 (2)	K(1)—O(4^{ii})	2.957 (4)	2.978 (6)	2.973 (5)
Ø	2.940		2.937	2.936	2.936
K(1)—O(2^{iv})	3.146 (2)	K(1)—O(2^{iii})	3.049 (9)	2.976 (5)	2.991 (5)
K(1)—O(2^{vii})	3.146 (2)	K(1)—O(4^{iii})	3.100 (16)	3.092 (10)	3.085 (10)
K(1)—O(2^{i})	3.146 (2)	K(1)—O(3^{iii})	3.258 (9)	3.376 (5)	3.368 (5)
Ø	3.146		3.139	3.148	3.148
Coordination of K(2)					
K(2)—O(2)	2.928 (2)	K(2)—O(2^{v})	2.945 (8)	2.973 (5)	2.965 (4)
K(2)—O(2^{v})	2.928 (2)	K(2)—O(2^{viii})	2.945 (8)	2.973 (5)	2.965 (4)
K(2)—O(2^{xv})	2.928 (2)	K(2)—O(3^{i})	2.868 (8)	2.827 (5)	2.830 (5)
K(2)—O(2^{xi})	2.928 (2)	K(2)—O(3)	2.868 (8)	2.827 (5)	2.830 (5)
K(2)—O(2^{xii})	2.928 (2)	K(2)—O(4^{vi})	2.951 (15)	2.971 (9)	2.976 (9)
K(2)—O(2^{xiii})	2.928 (2)	K(2)—O(4^{ii})	2.951 (15)	2.971 (9)	2.976 (9)
Ø	2.928		2.921	2.924	2.924
K(2)—O(1^{xviii})	3.3822 (1)	K(2)—O(1)	3.526 (11)	3.677 (6)	3.659 (6)
K(2)—O(1^{xix})	3.3822 (1)	K(2)—O(1^{vi})	3.384 (22)	3.357 (12)	3.362 (12)
K(2)—O(1)	3.3822 (1)	K(2)—O(1^{v})	3.225 (12)	3.113 (7)	3.124 (7)
K(2)—O(1^{xxi})	3.3822 (1)	K(2)—O(1^{i})	3.526 (11)	3.677 (6)	3.659 (6)
K(2)—O(1^{xv})	3.3822 (1)	K(2)—O(1^{ii})	3.384 (22)	3.357 (12)	3.362 (12)
K(2)—O(1^{xx})	3.3822 (1)	K(2)—O(1^{vii})	3.225 (12)	3.113 (7)	3.124 (7)
Ø	3.3822		3.378	3.382	3.382
Coordination of Na					
Na—O(2)	2.363 (2)	Na—O(2^{v})	2.349 (8)	2.349 (5)	2.355 (5)
Na—O(2^{xiv})	2.363 (2)	Na—O(2^{viii})	2.349 (8)	2.349 (5)	2.355 (5)
Na—O(2^{x})	2.363 (2)	Na—O(3^{ix})	2.368 (8)	2.389 (5)	2.389 (5)
Na—O(2^{xi})	2.363 (2)	Na—O(3)	2.368 (8)	2.389 (5)	2.389 (5)
Na—O(2^{xii})	2.363 (2)	Na—O(4^{vi})	2.360 (13)	2.347 (9)	2.341 (8)
Na—O(2^{xiii})	2.363 (2)	Na—O(4^{x})	2.360 (13)	2.347 (9)	2.341 (8)
Ø	2.359		2.359	2.362	2.362
Coordination of Cr					
Cr—O(1)	1.611 (5) (1.641)	Cr—O(1)	1.613 (3)	1.622 (3)	1.621 (3) (1.640)
Cr—O(2)	1.645 (2) (1.661)	Cr—O(2)	1.653 (8)	1.653 (5)	1.648 (5) (1.658)
Cr—O(2^{xvi})	1.645 (2) (1.661)	Cr—O(3)	1.650 (8)	1.644 (5)	1.644 (4) (1.654)
Cr—O(2^{xvii})	1.645 (2) (1.661)	Cr—O(4)	1.639 (11)	1.653 (6)	1.654 (7) (1.665)
O(1)—Cr—O(2)	110.41 (7)	O(1)—Cr—O(2)	109.7 (5)	109.9 (3)	109.6 (3)
O(1)—Cr—O(2^{xvi})	110.41 (7)	O(1)—Cr—O(3)	110.5 (5)	111.1 (3)	110.8 (3)
O(1)—Cr—O(2^{xvii})	110.41 (7)	O(1)—Cr—O(4)	111.3 (1.0)	111.3 (6)	111.0 (6)
O(2)—Cr—O(2^{xvi})	108.52 (6)	O(2)—Cr—O(3)	108.4 (4)	107.9 (3)	108.4 (3)
O(2)—Cr—O(2^{xvii})	108.52 (6)	O(2)—Cr—O(4)	108.3 (5)	108.4 (3)	108.3 (3)
O(2^{xvi})—Cr—O(2^{xvii})	108.52 (6)	O(3)—Cr—O(4)	108.6 (4)	109.0 (3)	108.7 (3)

Symmetry codes: for the high-temperature phase (290 K): (i) $x, y, z+1$; (ii) $-x, -y+1, -z+1$; (iii) $-x+1, -y+1, -z+1$; (iv) $-y+1, x-y+1, z+1$; (v) $y, -x+y, -z+1$; (vi) $y, -x+y+1, -z+1$; (vii) $-x+y, -x+1, z+1$; (viii) $x-y, x, -z+1$; (ix) $x-y+1, x+1, -z+1$; (x) $y, -x+y, -z$; (xi) $-y, x-y, z$; (xii) $-x+y, -x, z$; (xiii) $x-y, x, -z$; (xiv) $-x, -y, -z$; (xv) $-x, -y, -z+1$; (xvi) $-y+1, x-y+1, z$; (xvii) $-x+y, -x+1, z$; (xviii) $x-1, y-1, z$; (xix) $x, y-1, z$; (xx) $-x, -y+1, -z+1$; (xxi) $-x+1, -y+1, -z+1$.

For the low-temperature phase (230 and 200 K): (i) $-x, y, -z+\frac{1}{2}$; (ii) $-x+\frac{1}{2}, y-\frac{1}{2}, -z+\frac{1}{2}$; (iii) $x, -y+1, z+\frac{1}{2}$; (iv) $-x+\frac{1}{2}, y+\frac{1}{2}, -z+\frac{1}{2}$; (v) $x, y-1, z$; (vi) $x-\frac{1}{2}, y-\frac{1}{2}, z$; (vii) $-x, y-1, -z+\frac{1}{2}$; (viii) $-x, -y+1, -z$; (ix) $-x, -y, -z$; (x) $-x+\frac{1}{2}, -y+\frac{1}{2}, -z$.

Table 7. *Results of refinements for crystal A* (290 K) *carried out on data from separate* 60° *segments and its inversion counterparts of the reciprocal space*

The refinement conditions were otherwise the same as those in Table 1. The denomination of the segments is as follows:

$1(h \geq 0 \cap k \geq 0 \cap l \geq 0$ or $h \leq 0 \cap k \leq 0 \cap l \leq 0)$; $2(h \geq 0 \cap k \geq 0 \cap l \leq 0$ or $h \leq 0 \cap k \leq 0 \cap l \geq 0)$; $3(h \leq 0 \cap k \geq 0 \cap l \geq 0$; $|h| \leq k$ or $h \geq 0 \cap k \leq 0 \cap l \leq 0$; $|k| \geq h)$; $4(h \leq 0 \cap k \geq 0 \cap l \leq 0$; $|h| \leq k$ or $h \geq 0 \cap k \leq 0 \cap l \geq 0$; $|k| \geq h)$; $5(h \leq 0 \cap k \geq 0 \cap l \geq 0$; $|h| \geq k$ or $h \geq 0 \cap k \leq 0 \cap l \leq 0$; $|k| \leq h)$; $6(h \leq 0 \cap k \geq 0 \cap l \leq 0$; $|h| \geq k$ or $h \geq 0 \cap k \leq 0 \cap l \geq 0$; $|k| \leq h)$.

Segment	1	2	3	4	5	6
No. of reflections before/after averaging	506/238	506/238	504/237	504/237	503/237	503/237
R_{int}	0.0273	0.0296	0.0147	0.0197	0.0213	0.0254
R	0.0264	0.0413	0.0359	0.0264	0.0283	0.0260
wR	0.0373	0.0517	0.0450	0.0354	0.0364	0.0334
S	2.910	3.944	3.542	2.669	2.895	2.607
Twin fraction	0.537 (5)	0.529 (6)	0.511 (6)	0.512 (4)	0.546 (5)	0.547 (4)
Extinction correction g ($\times 10^{-4}$)	0.25 (3)	0.25 (4)	0.27 (3)	0.23 (2)	0.21 (2)	0.17 (2)

Table 8. *Results of refinements for crystal B* (200 K) *carried out on data from the separate symmetry-independent reciprocal space regions*

The refinement conditions were otherwise the same as those in Table 1. The denomination of the reciprocal space regions is as follows: $1(h \geq 0 \cap k \geq 0)$; $2(h \leq 0 \cap k \geq 0)$; $3(h \geq 0 \cap k \leq 0)$; $4(h \leq 0 \cap k \leq 0)$.

Segment	1	2	3	4
No. of reflections all/observed	1247/1179	1244/1178	1245/1179	1245/1187
R_{int} (all/observed)	0.0229/0.0208	0.0237/0.0216	0.0238/0.0217	0.0227/0.0210
R (all reflections)	0.0325	0.0330	0.0387	0.0291
R (observed reflections only)	0.0300	0.0306	0.0362	0.0271
wR (all reflections)	0.0413	0.0412	0.0485	0.0379
wR (observed reflections only)	0.0404	0.0403	0.0478	0.0372
S	1.698	1.665	1.960	1.559
Domain fractions				
f_1	0.140 (5)	0.157 (5)	0.162 (5)	0.143 (5)
f_2	0.134 (5)	0.138 (4)	0.144 (5)	0.133 (4)
f_3	0.126 (4)	0.112 (5)	0.117 (5)	0.125 (4)
f_4	0.211 (4)	0.197 (4)	0.180 (4)	0.207 (4)
f_5	0.188 (4)	0.187 (5)	0.175 (5)	0.186 (4)
f_6	0.201 (5)	0.209 (4)	0.222 (5)	0.206 (5)
$f_1 + f_3 + f_5$	0.454	0.456	0.454	0.454
$f_2 + f_4 + f_6$	0.546	0.544	0.546	0.546

Table 9. *Results of refinements for crystal A* (200 K) *carried out on data from the separate symmetry-independent reciprocal space regions*

The refinement conditions were otherwise the same as those in Table 1. The denomination of the reciprocal space regions is as follows: $1(h \geq 0 \cap k \geq 0)$; $2(h \leq 0 \cap k \geq 0)$; $3(h \geq 0 \cap k \leq 0)$; $4(h \leq 0 \cap k \leq 0)$. Cr($i$) and Cr($a$) indicate the variants with respective isotropic and anisotropic refinement of Cr atoms.

Reciprocal region	1	2	3	4
No. of reflections all/observed	1245/1215	1242/1207	1241/1211	1247/1218
R_{int} (all/observed)	0.0113/0.0107	0.0114/0.0107	0.0114/0.0108	0.0111/0.0106
R (all reflections); Cr(i)/Cr(a)	0.0358/0.0353	0.0307/0.0295	0.0307/0.0290	0.0392/0.0372
R (observed reflections only); Cr(i)/Cr(a)	0.0349/0.0344	0.0296/0.0285	0.0298/0.0281	0.0383/0.0364
wR (all reflections); Cr(i)/Cr(a)	0.0537/0.0534	0.0478/0.0472	0.0492/0.0482	0.0548/0.0538
wR (observed reflections only); Cr(i)/Cr(a)	0.0536/0.0533	0.0476/0.0470	0.0491/0.0481	0.0546/0.0536
S	3.341/3.331	2.952/2.925	3.043/2.986	3.431/3.374
Domain fractions				
f_1 Cr(i)/Cr(a):	0.148 (5)/0.147 (5)	0.151 (5)/0.148 (5)	0.203 (5)/0.205 (5)	0.177 (5)/0.183 (5)
f_2 Cr(i)/Cr(a):	0.152 (6)/0.145 (6)	0.148 (5)/0.145 (5)	0.158 (5)/0.160 (5)	0.151 (6)/0.167 (5)
f_3 Cr(i)/Cr(a)	0.136 (5)/0.136 (5)	0.176 (4)/0.176 (4)	0.158 (5)/0.157 (5)	0.187 (6)/0.191 (6)
f_4 Cr(i)/Cr(a)	0.225 (5)/0.228 (5)	0.208 (4)/0.211 (4)	0.175 (4)/0.171 (4)	0.166 (5)/0.155 (4)
f_5 Cr(i)/Cr(a)	0.115 (5)/0.118 (5)	0.124 (5)/0.127 (5)	0.113 (5)/0.111 (5)	0.115 (5)/0.103 (5)
f_6 Cr(i)/Cr(a):	0.224 (6)/0.226 (6)	0.193 (5)/0.193 (5)	0.193 (5)/0.196 (5)	0.204 (6)/0.201 (6)
$f_1 + f_3 + f_5$ Cr(i)/Cr(a):	0.399/0.401	0.451/0.451	0.474/0.473	0.479/0.477
$f_2 + f_4 + f_6$ Cr(i)/Cr(a):	0.601/0.599	0.549/0.549	0.526/0.527	0.521/0.523
Extinction correction g ($\times 10^{-4}$)	0.062 (12)/0.061 (12)	0.062 (10)/0.064 (11)	0.064 (11)/0.069 (11)	0.070 (12)/0.076 (13)

space (Table 7). Similar calculations were carried out on the 200 K data of crystals *A* and *B* (Tables 8 and 9).

The result of the room-temperature phase (crystal *A*) refinement has shown that the atomic coordinates are almost independent of the data-set choice (within 2 e.s.d.'s) but the refined twin-fraction parameters changed significantly.

A similar result was yielded by the refinement of the ferroelastic phases: the differences between atomic coordinates are within 5 e.s.d.'s but the values of domain fractions are strongly dependent on the symmetry-independent data-set choice. It is worthwhile noting that the refinement of the low-temperature phases had to be performed with damping in order to reach convergence with $\Delta/\sigma < 0.02$.

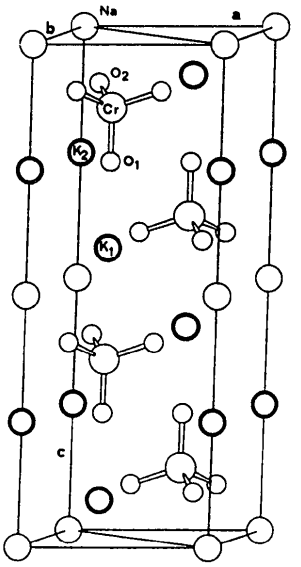

Fig. 2. Trigonal phase of $K_3Na(CrO_4)_2$. Two unit cells which are linked by the lattice translation along the *c* axis are depicted.

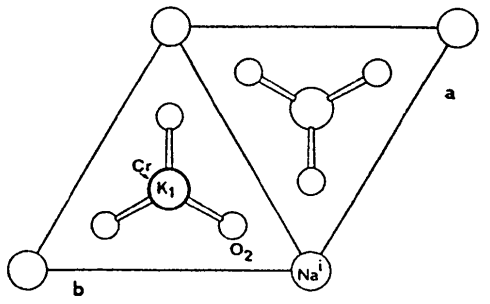

Fig. 3. View of the trigonal phase of $K_3Na(CrO_4)_2$ along the *c* axis (the symmetry code is given in Table 6).

Comparison of Tables 7 and 8 indicates that in the case of crystal *B* the sums of $f_1 + f_3 + f_5$ and $f_2 + f_4 + f_6$ are not affected by the choice of data set.

As already stated above, the transition into *C*2/*c* should conserve the sum of domain fractions within each 120° domain pattern. The sum of the domain fractions of the low-temperature phases of crystal *A* ($f_2 + f_4 + f_6$, Table 1) are 0.558 and 0.551 for 230

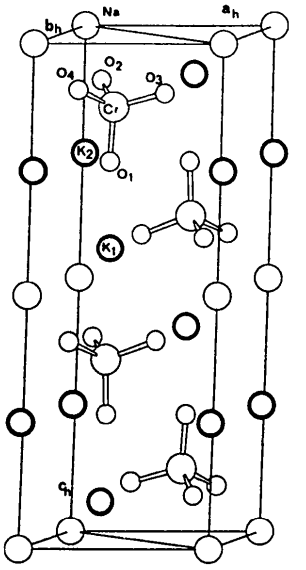

Fig. 4. Monoclinic phase of $K_3Na(CrO_4)_2$ at 230 K. The structure is depicted in the pseudo-hexagonal unit cell ($a_h = -a_m/2 - b_m/2$; $b_h = a_m/2 - b_m/2$; $c_h = c_m$; *h*, *m* indices apply for the pseudo-hexagonal and monoclinic cells, respectively). The coordinates of all signed atoms in the pseudo-hexagonal unit cell except Na are connected with the coordinates given in Table 4 by the transformation $x_h = -x_m - y_m + 1$, $y_h = x_m - y_m + 1$, $z_h = z_m$; the coordinates of the Na by the transformation $x_h = -x_m - y_m$, $y_h = x_m - y_m$, $z_h = z_m$.

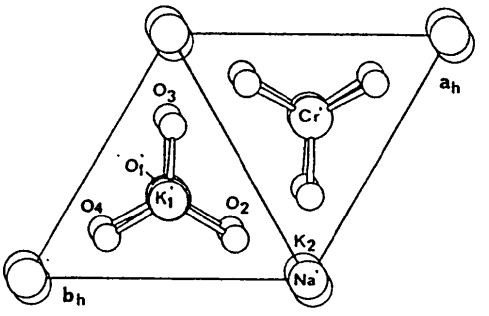

Fig. 5. View along the *c* axis of the monoclinic phase of $K_3Na(CrO_4)_2$ at 230 K. The structure is depicted in the pseudo-hexagonal cell – see comments to Fig. 4. The coordinates of Cr', K_1' and Na' are connected with the pertinent atoms depicted in Fig. 4 by the transformations: $(1 - x_h, 1 - y_h, 1 - z_h)$, $(1 - y_h, 1 - x_h, \frac{1}{2} + z_h)$, $(x_h, y_h, 1 + z_h)$, respectively.

and 200 K, respectively. This seems to be a non-negligible deviation from the value $f_2 = 0.532$ calculated for the room-temperature phase (the constrained refinement of domains $f_2 + f_4 + f_6 = 0.532$ gave an R-factor value about 0.002 higher).

This peculiarity, however (Tables 7–9), may be explained by the effect of the mutual shielding of domains and by the errors in absorption correction, and the monoclinic symmetry was assumed as in $K_3Na(SeO_4)_2$ (Fábry, Breczewski & Petricek, 1993).

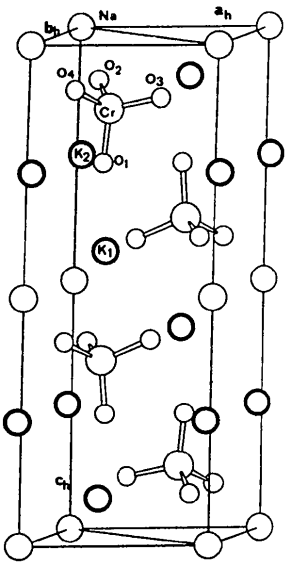

Fig. 6. Monoclinic phase of $K_3Na(CrO_4)_2$ at 200 K. The structure is depicted in the pseudo-hexagonal unit cell ($a_h = -a_m/2 - b_m/2$; $b_h = a_m/2 - b_m/2$; $c_h = c_m$; h, m indices apply for the pseudo-hexagonal and monoclinic cells, respectively). The coordinates of the signed atoms are connected with the coordinates given in Table 5 in the same way as in Fig. 4.

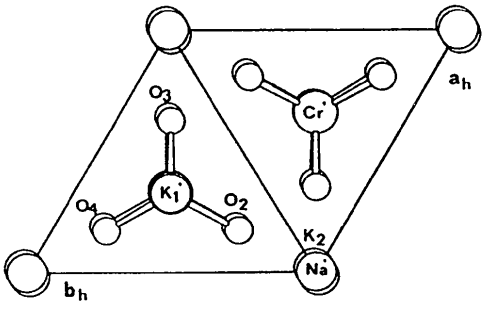

Fig. 7. View along the c axis of the monoclinic phase of $K_3Na(CrO_4)_2$ at 200 K. The structure is depicted in the pseudo-hexagonal cell – see comments to Fig. 6. The coordinates of Cr′, K_1′, Na′ and O_1′ are connected with the pertinent atoms depicted in Fig. 6 by the transformations $(1 - x_h, 1 - y_h, 1 - z_h)$, $(1 - y_h, 1 - x_h, \frac{1}{2} + z_h)$, $(x_h, y_h, 1 + z_h)$ and $(1 - y_h, 1 - x_h, \frac{1}{2} + z_h)$, respectively.

Table 10. *Absolute values of displacement vectors Δ (Å) with e.s.d.'s in parentheses*

A and *B* indexed atoms denote the atoms from the domains related by rotation in an anticlockwise direction by 120 and 240°, respectively.

	A (200 K) $\lvert\Delta\rvert$	*B* (200 K) $\lvert\Delta\rvert$	*A* (230 K) $\lvert\Delta\rvert$
K(1)—$K(1)_A$	0.115 (1)	0.111 (1)	0.059 (2)
K(1)—$K(1)_B$	0.115 (2)	0.111 (2)	0.058 (4)
$K(1)_A$—$K(1)_B$	0.114 (2)	0.109 (2)	0.061 (4)
K(2)—$K(2)_A$	0.303 (1)	0.320 (1)	0.166 (1)
K(2)—$K(2)_B$	0.303 (1)	0.320 (1)	0.166 (1)
$K(2)_A$—$K(2)_B$	0.303 (1)	0.320 (1)	0.166 (1)
Cr—Cr_A	0.094 (1)	0.087 (2)	0.050 (2)
Cr—Cr_B	0.096 (1)	0.089 (2)	0.048 (2)
Cr_A—Cr_B	0.094 (1)	0.087 (2)	0.051 (2)
O(1)—$O(1)_A$	0.256 (12)	0.241 (11)	0.133 (15)
O(1)—$O(1)_B$	0.255 (12)	0.240 (11)	0.135 (21)
$O(1)_A$—$O(1)_B$	0.257 (13)	0.242 (12)	0.132 (24)
O(2)—$O(4)_A$	0.226 (8)	0.205 (7)	0.110 (13)
O(2)—$O(3)_B$	0.357 (7)	0.333 (7)	0.184 (13)
$O(3)_B$—$O(4)_A$	0.281 (9)	0.279 (10)	0.154 (15)
O(3)—$O(2)_A$	0.356 (7)	0.333 (7)	0.185 (12)
O(3)—$O(4)_B$	0.282 (10)	0.280 (11)	0.152 (17)
$O(2)_A$—$O(4)_B$	0.226 (7)	0.204 (6)	0.111 (12)
O(4)—$O(2)_B$	0.228 (9)	0.206 (8)	0.108 (13)
O(4)—$O(3)_A$	0.282 (10)	0.279 (10)	0.154 (16)
$O(2)_B$—$O(3)_A$	0.356 (6)	0.332 (7)	0.185 (11)

It should be noted that the extinction correction applied for crystal *A* may be linked with the effect of domain shielding. Since the atomic temperature factors of crystal *B* are realistic and the extinction correction in this crystal turned out to be insignificant, the structure determination of crystal *B* should be preferred. The differences in coordinates (Table 5) indicate that the real accuracy of the experiment is of the order of the second decimal place in fractional coordinates.

The present results have shown that the phase transition in $K_3Na(CrO_4)_2$ is continuous with gradually increasing atomic displacements (when lowering the temperature) from positions in the $P\bar{3}m1$ parent phase. The growing atomic displacements are accompanied by a gradually increasing inclination of the anion tetrahedra: the angles between the Cr—O(1) bond and the c^*-axis direction are 3.74° at 230 K and 7.16 and 6.71° at 200 K for crystals *A* and *B*, respectively.

The values of atomic displacement vectors (Table 10) at 200 K are very similar to those in $K_3Na(SeO_4)_2$ at 291 K (Fábry, Breczewski & Petricek, 1993).

Visual comparison of precession photographs of $K_3Na(SeO_4)_2$ showed that the intensities of the newly developed reflections in the monoclinic phase also increase gradually with decreasing temperature. However, this change is rather limited to the much narrower temperature interval between 334 and 346 K (the phase-transition point) (Fábry, Breczewski & Petricek, 1993; Krajewski, Mroz & Piskunowicz, 1993).

The authors (JF and TB) gratefully acknowledge the support of the DGCYT of the Spanish Ministry of Education and Science. This work was supported by the UPV project No. 063.310-E160/90. The referee is also thanked for his suggestions.

References

ABRAHAMS, S. C. & KEVE, E. T. (1971). *Ferroelectrics*, **2**, 129–154.
BECKER, P. J. & COPPENS, P. (1974). *Acta Cryst.* A**30**, 129–141.
BUSING, W. R. & LEVY, H. A. (1964). *Acta Cryst.* **17**, 142–146.
COSIER, J. & GLAZER, A. M. (1986). *J. Appl. Cryst.* **19**, 105–107.
CROMER, D. T. & MANN, J. B. (1968). *Acta Cryst.* A**24**, 129–144.
FÁBRY, J., BRECZEWSKI, T. & PETRICEK, V. (1993). *Acta Cryst.* Submitted.
KRAJEWSKI, T., MROZ, B. & PISKUNOWICZ, P. (1993). *Phys. Status Solidi A*, **135**, 557–564.
KRAJEWSKI, T., MROZ, B., PISKUNOWICZ, P. & BRECZEWSKI, T. (1990). *Ferroelectrics*, **106**, 225–230.
MADARIAGA, G. & BRECZEWSKI, T. (1990). *Acta Cryst.* C**46**, 2019–2021.
MROZ, B., KIEFTE, H., CLOUTER, M. J. & TUSZYNSKI, J. A. (1991). *Phys. Rev. B*, **43**, 641–648.
NARDELLI, M. (1983). *Comput. Chem.* **7**, 95–98.
OKADA, K. & OSSAKA, J. (1980). *Acta Cryst.* B**36**, 919–921.
PETRICEK, V. & MALY, K. (1988). *The SDS System. Program Package for X-ray Structure Determination.*
STEWART, J. M., KRUGER, G. J., AMMON, H. L., DICKINSON, C. W. & HALL, S. R. (1972). *The XRAY72 System.* Version of June 1972. Technical Report TR-192. Computer Science Center, Univ. of Maryland, College Park, Maryland, USA.

Acta Cryst. (1994). B**50**, 22–30

Crystalline Phases Related to a Decagonal Quasicrystal. I. A Single-Crystal X-ray Diffraction Study of the Orthorhombic Al_3Mn Phase

BY N. C. SHI

X-ray Laboratory, China University of Geosciences, 100083 *Beijing, People's Republic of China*

X. Z. LI

Beijing Laboratory of Electron Microscopy, Chinese Academy of Sciences, 100080 *Beijing, People's Republic of China*

Z. S. MA

X-ray Laboratory, China University of Geosciences, 100083 *Beijing, People's Republic of China*

AND K. H. KUO*

Beijing Laboratory of Electron Microscopy, Chinese Academy of Sciences, 100080 *Beijing, People's Republic of China*

(*Received* 13 *April* 1993; *accepted* 16 *August* 1993)

Abstract

Al_3Mn (with the stoichiometric composition $Al_{28.1}Mn_{10.9}$), $M_r = 1356.5$, orthorhombic, $Pn2_1a$, $a = 14.837$ (4), $b = 12.457$ (2), $c = 12.505$ (2) Å, $V = 2311.2$ (8) Å^3, atoms/cell = 4×39, $D_x = 3.90$ g cm^{-3}, λ(Mo $K\alpha$) = 0.71069 Å, $\mu = 65.82$ cm^{-1}, $F(000) = 2550.15$, room temperature, $R = 0.068$ for 1289 reflections. About two-thirds of Mn atoms have icosahedral coordination. In a repeat unit b, there are four interpenetrated icosahedra with two Mn and two Al atoms at their centers. This phase has a layer structure consisting of an almost 'flat' layer F sandwiched between two puckered P and p layers in the sequence $PFpP'F'p'$..., where $P'F'p'$ and PFp are related by the 2_1 axes parallel to [010]. A similar layer structure has also been found in the π-AlMnM (M = Ni, Cu, Zn) phases. Both these two crystalline structures can be obtained from that of the Al–Mn decagonal quasicrystal by substituting a rational ratio of two consecutive Fibonacci numbers for the irrational $\tau = [1 + (5)^{1/2}]/2$ in the two quasiperiodic directions.

1. Introduction

Soon after the discovery of the first icosahedral quasicrystal with $m35$ point-group symmetry, it was found that the quasicrystal and the crystalline phase of a similar composition generally have the same or

* Correspondence author: PO Box 2724, 100080 Beijing, People's Republic of China.